Determination of consecutive bond energies by photoionization of SbH_n ($n=1$–3)

B. Ruscic and J. Berkowitz
Chemistry Division, Argonne National Laboratory, Argonne, Illinois 60439

(Received 2 June 1993; accepted 29 June 1993)

A photoionization mass spectrometric study of SbH_3 is presented. The adiabatic ionization potential (IP) of SbH_3 is $\leqslant 9.40 \pm 0.02$ eV. The lowest energy fragment ion, SbH^+ $(+H_2)$, has an appearance potential (0 K) of $9.73_0 \pm 0.00_8$ eV, while SbH_2^+ has an AP of 11.66 ± 0.02 eV. The transient species SbH_2 and SbH are generated *in situ* by reacting F atoms with SbH_3. The IP of SbH_2, forming SbH_2^+ ($X\,^1A_1$), is 8.731 ± 0.012 eV. The IP of SbH ($X\,^3\Sigma^-,0^+$) to form SbH^+ ($X\,^2\Pi_{1/2}$) is probably 8.753 ± 0.009 eV, but certainly < 8.79 eV. Autoionizing structure in the photoion yield curve of SbH^+ (SbH) is interpreted as Rydberg series converging to SbH^+ ($a\,^4\Sigma^-$), which appears to be split into 1/2 and 3/2 components, with IP's of 10.843 ± 0.011 eV and 10.866 ± 0.011 eV. The difference in IP's (Sb–SbH, SbH–SbH_2) appears to conform to the extended Goddard–Harding model, when adjusted for spin–orbit splittings. The derived heats of formation are $\Delta H^0_{f0}(SbH) = 59.1 \pm 0.3$ kcal/mol and $\Delta H^0_{f0}(SbH_2) = 52.5 \pm 0.6$ kcal/mol. These values lead to $D_0(SbH) = 56.4 \pm 1.0$, $D_0(HSb–H) = 58.3 \pm 0.6$, $D_0(H_2Sb–H) = 67.5 \pm 0.5$ (in kcal/mol). The differences in successive bond energies, 1.9 ± 1.2 and 9.2 ± 0.8 kcal/mol, depart significantly from the constant value (4.44 kcal/mol) predicted by the Goddard–Harding model. A rationalization is presented, that incorporates relativistic effects. This relativistic picture implies that for BiH_n, $D_0(BiH) > D_0(HBi–H)$, a conclusion for which some experimental evidence exists. However, relativistic *ab initio* calculations, which agree rather well in their calculated differences in successive bond energies for SbH_n, do not predict this reversal in BiH_n.

I. INTRODUCTION

Antimony is one of the Group V (pnicogen, Pn) elements utilized to form semiconductors of the III–V compounds, e.g., gallium antimonide and indium antimonide. It has been tested as a dopant in the new class of high temperature superconductors. Volatilization of solid antimony generates the tetramer (Sb_4) preponderantly. If one desires Sb or Sb_2 beams, it may be more desirable to decompose stibine (SbH_3). However, very little is known experimentally about the Sb–H bond energies in SbH_3.

The atomization energy of SbH_3 can be deduced from $\Delta H^0_f(SbH_3)$, ΔH^0_f (Sb,g), and ΔH^0_f(H). With $\Delta H^0_{f298}(SbH_3) = 34.61 \pm 0.10$ kcal/mol,[1] [ΔH^0_{f0} $(SbH_3) = 36.54 \pm 0.10$ kcal/mol], $\Delta H^0_{f0}(Sb,g) = 63.8 \pm 1.0$ kcal/mol,[2] and $\Delta H^0_{f0}(H) = 51.634$ kcal/mol, one obtains an atomization energy of 182.2 ± 1.0 kcal/mol, or an average bond energy of 60.7 kcal/mol. Goddard and Harding[3] developed a semiempirical model, based on the assumption of purely covalent behavior and the counting of p–p' exchange integrals before and after bond formation, to predict the consecutive bond energies in Group V and Group VI hydrides. This model involves two nonadjustable parameters—the aforementioned atomization energy, and the magnitude of K, the p–p' exchange integral, obtained from atomic spectra. For Sb, the energy difference (weighted statistically) between the ground state (^4S) and the first excited state (^2D) is 9317.5 cm^{-1},[4] and corresponds to 3 K. The Goddard–Harding model predicts a difference between consecutive bond energies of $K/2 = 4.44$ kcal/mol. Thus $D_0(Sb–H) = 56.3$ kcal/mol, $D_0(HSb–H) = 60.7$ kcal/mol, and $D_0(H_2Sb–H) = 65.2$ kcal/mol. [These values differ somewhat from the original ones of Goddard and Harding,[3] reflecting a new $\Delta H^0_{f0}(Sb,g)$]. *Ab initio* theory, which has been applied to the lighter Group V and Group VI hydrides with some success[5] (deviation from experimental bond energies of $\leqslant 2$ kcal/mol) becomes a formidable task for elements as heavy as Sb. Dai and Balasubramanian[6] have employed a complete active space multiconfiguration self-consistent field (CASSCF) followed by full second order configuration interaction (SOCI) to calculate various properties of AsH_n, SbH_n, and BiH_n($n=1$–3), including consecutive bond energies and individual ionization potentials. In these calculations, spin–orbit coupling is taken into account using a relativistic configuration interaction (RCI) scheme. They report $D_0(Sb–H) = 53.9$ kcal/mol, $D_0(HSb–H) = 55.8$ kcal/mol and $D_0(H_2Sb–H) = 63.3$ kcal/mol. These bond energies are smaller than the values predicted by the Goddard–Harding model, and the difference between consecutive bond energies is not constant. The first two bonds are closer in energy, the third bond significantly larger. Such a trend could already be seen in previous work from this laboratory on AsH_n.[7] The differences $D_0(H_2As–H)$-$D_0(HAs–H)$ and $D_0(HAs–H) - D_0(As–H)$ were 8.4 and 1.9 kcal/mol, respectively, whereas Goddard and Harding predicted a constant value of 5.15 kcal/mol. The departure from this constant difference was less apparent for the phosphorus hydrides.[8] One issue we wished to explore in the current research was this deviation: was it real, was it progressive, did it herald the influence of spin–orbit or other relativistic effects? Spectroscopic information is lacking. The Huber–Herzberg compilation[9] has no value for $D_0(SbH)$, nor have we been able to find a value in subsequent literature.

 0021-9606/93/99(8)/5840/9/$6.00

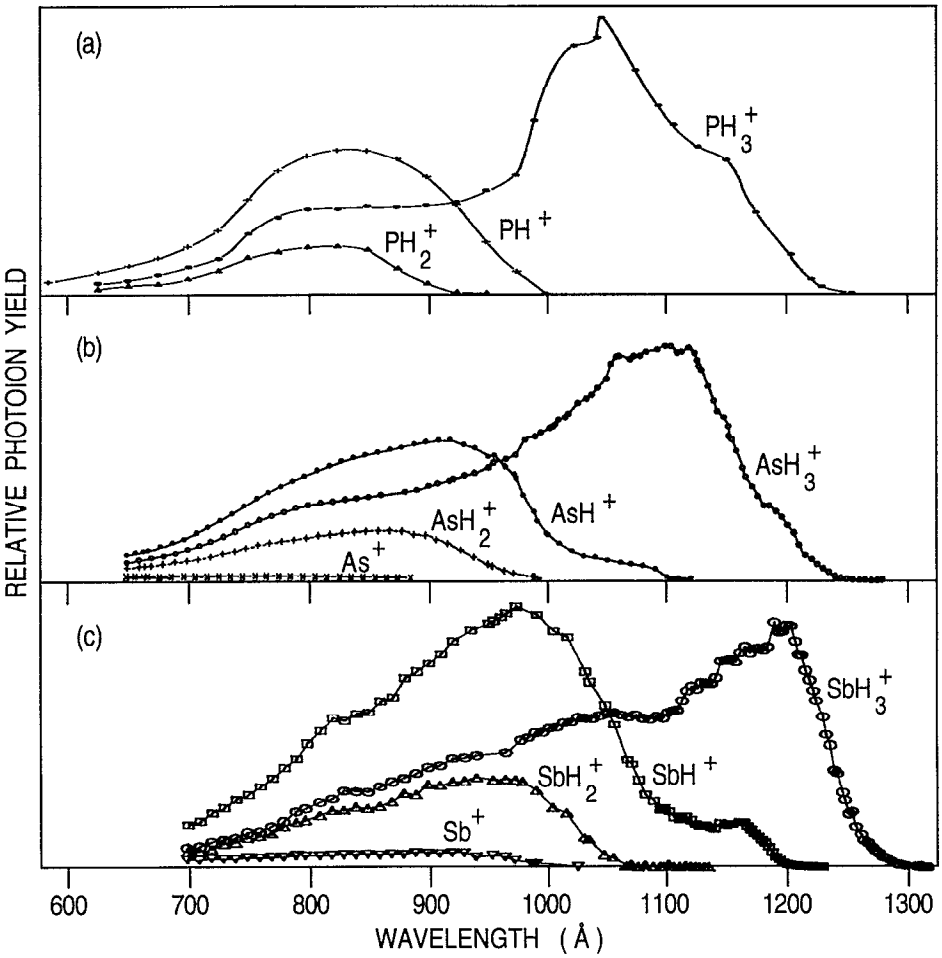

FIG. 1. (a) Photoion yield curves of parent and fragment ions from PH_3 [from Ref. 8(a)]; (b) photoion yield curves of parent and fragment ions from AsH_3 (from Ref. 9); (c) photoion yield curves of parent and fragment ions from SbH_3 (present results).

II. EXPERIMENTAL ARRANGEMENT

The approach to be used here, similar to earlier work on PH_n (Ref. 8) and AsH_n (Ref. 9) species, was to prepare SbH_2 and SbH, *in situ*, by successive H atom abstraction from SbH_3. In the earlier work, it was found that reaction of PH_3 and AsH_3 with H atoms provided the desired intensity of the transient species. In the present studies, it was found necessary to use F atoms as the reagent, since the H atom reactions did not produce a satisfactory yield. With this reaction, it was possible to generate measurable quantities of SbH_2, SbH, and even Sb.

SbH_3 was prepared by the method of Jolly and Drake.[10] The product, after distillation, was maintained as a solid in a toluene slush bath to avoid potential hazards associated with liquid SbH_3. The sublimed vapor provided sufficient pressure for the experiments at hand. The reactor employed for generating the transient species was identical to that used in prior F atom reaction studies in this laboratory.

Vacuum ultraviolet photoionization studies were performed on SbH_3, SbH_2, and SbH. With the relatively stable SbH_3, the gas flowed into a more enclosed chamber for interaction with the dispersed vacuum ultraviolet radiation, whereas the studies on the transient species were performed with an "open" chamber, permitting the crude molecular beam to pass into and through the ionization chamber with very few wall collisions. The basic apparatus consisting of a tunable vuv light source, an ionization region, and a mass spectrometer to identify the ions of interest, has been described previously.[11,12] The bandwidth of the vuv monochromator for these experiments was 0.84 Å (FWHM).

III. EXPERIMENTAL RESULTS

A. SbH_3

The ions SbH_3^+, SbH_2^+, and SbH^+ were observed with sufficient intensity for detailed study. An overview of their photoion yield curves from the onset of ionization to 700 Å is shown in Fig. 1(c). The Sb^+ fragment is also shown in this figure, although its threshold is not expected to have thermochemical significance. Although SbH_3^+, SbH_2^+, SbH^+, and Sb^+ were measured at $m/e=126$, 125, 122, and 121, respectively, the curves in Fig. 1(c) have been corrected for isotopic composition. The parent ion, SbH_3^+, increases gradually in intensity from threshold. This is con-

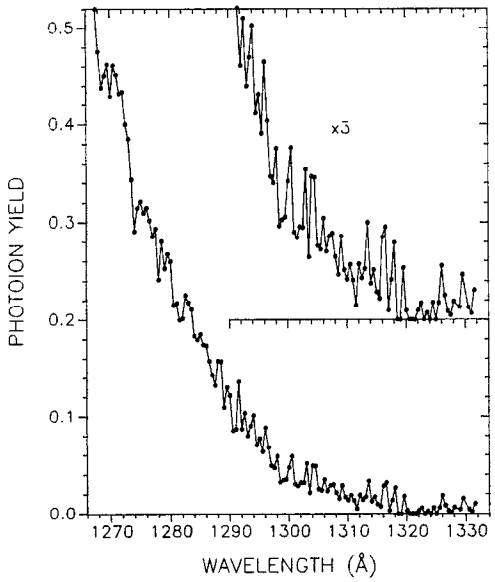

FIG. 2. The threshold region for formation of the parent ion SbH_3^+ from SbH_3.

sistent with photoelectron spectroscopic results,[13] where it was concluded that the transition was from pyramidal SbH_3 to a much less pyramidal (but not quite planar) SbH_3^+. The lowest energy fragment, SbH^+ $(+H_2)$ begins to appear weakly, and with a shallow slope at ~1280 Å. It experiences an increase in slope at ~1200 Å, but does not exceed the intensity of the parent ion until ~1050 Å. Comparison with the corresponding fragmentation behavior of PH_3 [Ref. 8(a)] and AsH_3 (Ref. 9) is revealing [Figs. 1(a) and 1(b)]. In PH_3, the PH^+ fragment increases rather abruptly at threshold, and surpasses the parent ion in abundance within ~70 Å of the PH^+ onset. In AsH_3, the AsH^+ ion increases more gradually from threshold, then manifests an increase in slope at higher energy, and exceeds the parent ion's abundance about 140 Å from the AsH^+ onset. With SbH_3, the initial slope of SbH^+ is very shallow, and its intensity begins to exceed that of SbH_3^+ about 230 Å beyond the SbH^+ onset. This pattern may be related to the increasing H–H distances in PH_3^+, AsH_3^+, and SbH_3^+, making H_2 formation more difficult, i.e., a more constrained transition state. The SbH_2^+ fragment begins to appear at ~1080 Å, and does not exceed the intensity of either SbH^+ or SbH_3^+ in the wavelength region studied. This parallels the behavior of PH_2^+ and AsH_2^+.

1. SbH_3^+

In Fig. 2, an amplified version of the threshold region for SbH_3^+ (SbH_3) is displayed with a larger point density. The first detectable departure from the background level in the gradually ascending curve occurs at ~1319±3 Å≡9.40±0.02 eV. The adiabatic ionization potential (IP) obtained from HeI photoelectron spectroscopy[13] was 9.51 eV. Some rounded step structure, indicative of direct ionization to successive vibrational levels of the inversion mode of SbH_3^+, is evident.

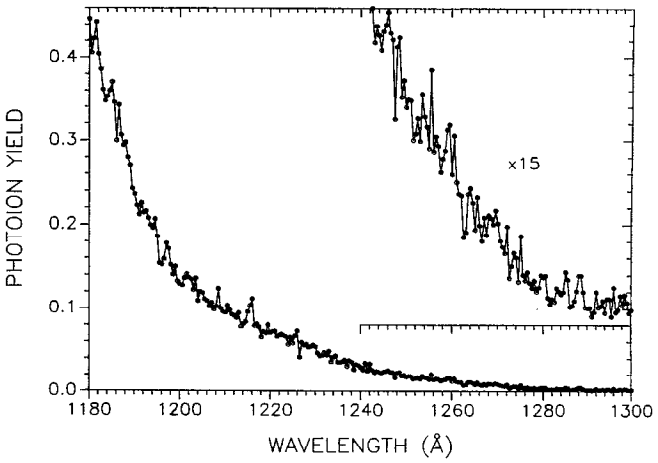

FIG. 3. The threshold region for formation of SbH^+ $(+H_2)$ from SbH_3.

2. SbH^+

An enlarged version of the threshold region for SbH^+ (SbH_3), with a larger point density, appears in Fig. 3. The appearance potential (AP), obtained by extrapolation of the initial quasilinear section (shown in the inset of Fig. 3), is 1280±1 Å≡9.68_6±0.008 eV. When corrected for the internal thermal energy of SbH_3,[14] one obtains 9.73_0 ±0.008 eV as the 0 K threshold.

3. SbH_2^+

A more detailed and magnified plot of the threshold region for SbH_2^+ (SbH_3) is shown in Fig. 4. The photoion yield curve increases approximately linearly below ~1060 Å. This linear portion, extrapolated to the background level, intersects it at 1067±2 Å≡11.62±0.02 eV. Upon correction for the internal thermal energy of SbH_3 at 298 K, the equivalent 0 K threshold becomes 11.66±0.02 eV.

B. SbH_2

Some SbH_2^+ (SbH_2) was observed in an experiment involving the H+SbH_3 reaction, but a stronger signal was

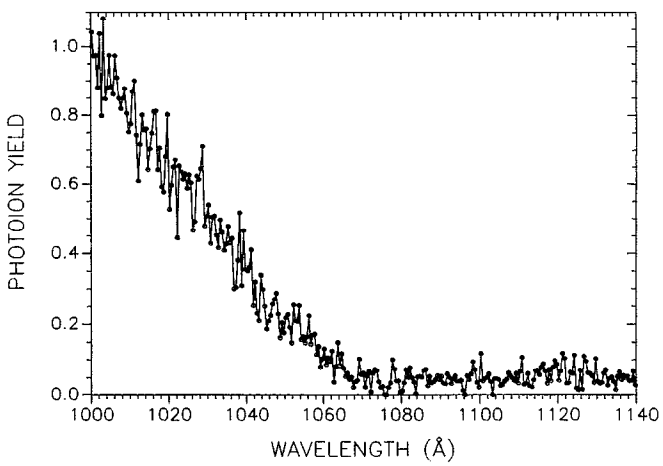

FIG. 4. The threshold region for formation of SbH_2^+ from SbH_3.

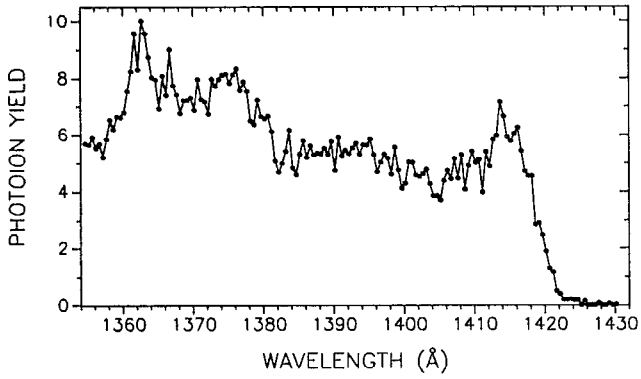

FIG. 5. Photoion yield curve of SbH_2^+ from SbH_2. The SbH_2 is generated *in situ* by the reaction of F with SbH_3.

obtained in the $F+SbH_3$ reaction. The photoion yield curve of $SbH_2^+(SbH_2)$ is presented in Fig. 5 from the onset of ionization to ~1350 Å. The variation of ion yield with wavelength over the entire scan bears a coarse resemblance to that of PH_2^+ (PH_2) (Ref. 8) and AsH_2^+ (AsH_2),[7] but is distinctly different from NH_2^+ (NH_2).[15] In the latter curve, for the first 100 Å above the ionization threshold there are sharp, intense ionization features superimposed upon a gradually rising continuum. These sharp features are components of a Rydberg series converging to the first excited state of the ion, $^1A_1$, whereas the gradually rising continuum represents formation of the ionic ground state, $^3B_1$. By contrast, $PH_2^+(PH_2)$, $AsH_2^+(AsH_2)$, and $SbH_2^+(SbH_2)$ have in common a relatively sharp onset, and then a plateau with relatively mild and broad undulations. In the $SbH_2^+(SbH_2)$ spectrum, one can recognize broad autoionizing features at ~1414, 1376, and 1363 Å, as well as less prominent ones. Corresponding features in PH_2^+ and AsH_2^+, obtained with better resolution and signal-to-noise ratios, have not yet been assigned. However, the overall pattern is consistent with the interpretation of the ground state being $^1A_1$ for SbH_2^+, as was found for AsH_2^+ and PH_2^+, but not NH_2^+. In all of these systems, the neutral species in its electronic ground state is strongly bent (NH_2,[16] 103°20′; PH_2,[17] 93.4°; AsH_2,[6] 90.7°; SbH_2,[6] 89.8°) as are the $^1A_1$ states of the cations (NH_2^+,[18] 110.0°; PH_2^+,[18] 94.4°; AsH_2^+,[19] 91.4°; SbH_2^+,[19] 90.7°). However, the $^3B_1$ states of the cations have more obtuse angles (NH_2^+,[18,20] 150.9°, quasilinear; PH_2^+,[18] 121.4°; AsH_2^+,[19] 121.8°, SbH_2^+,[19] 119.8°). Consequently, the Franck–Condon factors may be expected to be more favorable for ionization to the $^1A_1$ state (narrow Franck–Condon band, sharp feature) than for ionization to the $^3B_1$ state (broad Franck–Condon band). The sharp autoionizing Rydberg features in the spectrum of NH_2^+ (NH_2), which converge to the excited state of NH_2^+, imply that this excited state is $^1A_1$. The gradually rising continuum reflects the broad Franck–Condon distribution for formation of the ionic ground state, which is $^3B_1$. The relatively abrupt threshold behavior of PH_2^+, AsH_2^+, and SbH_2^+, and the absence of sharp autoionizing features, is evidence that the ground states of these cations may be characterized as $^1A_1$. The $X\,^1A_1$–$a\,^3B_1$ splitting is not yet known experimentally, but has been calculated to be 0.92 eV (PH_2^+),[18] 0.95 eV (AsH_2^+),[19] and 1.08 eV (SbH_2^+).[19]

If the wavelength range of the initial ascent in the photoion yield curve represents the rotational breadth of the transition, then it may be possible to fit this portion of the curve, utilizing the moments of inertia of neutral and cation, and the temperature. In this way, it was possible to select the rotational zero–zero transition, and hence the adiabatic IP of PH_2.[8(a)] In the present case, the required moments of inertia are not fully known, and the data have more statistical uncertainty. Hence, by analogy with PH_2 (AsH_2), we approximate the zero–zero transition as the half-rise point, and (allowing for a more generous uncertainty), the adiabatic IP of SbH_2 to form SbH_2^+, $X\,^1A_1$, is 1420 ± 2 Å $\equiv 8.731\pm0.012$ eV.

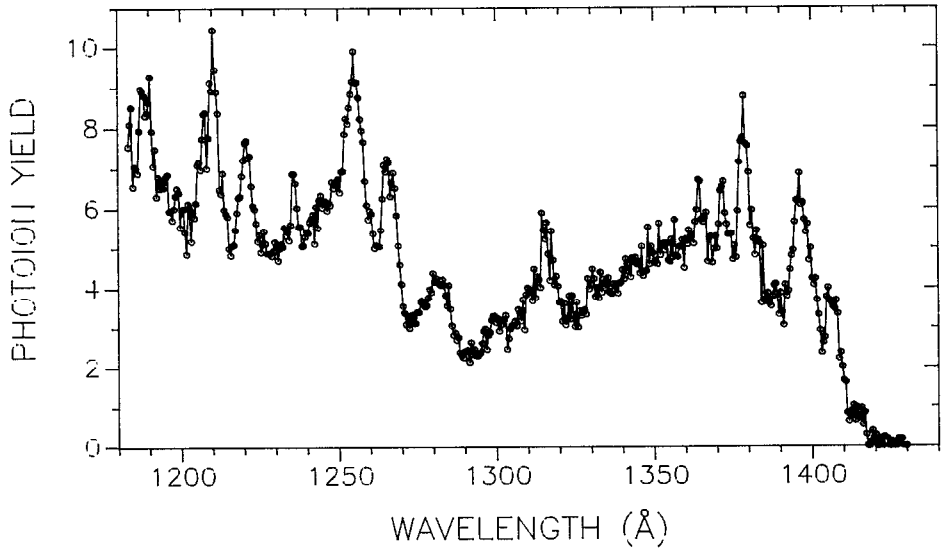

FIG. 6. Photoion yield curve of SbH^+ from SbH. The SbH species is generated *in situ*, perhaps by successive reactions of F with SbH_3.

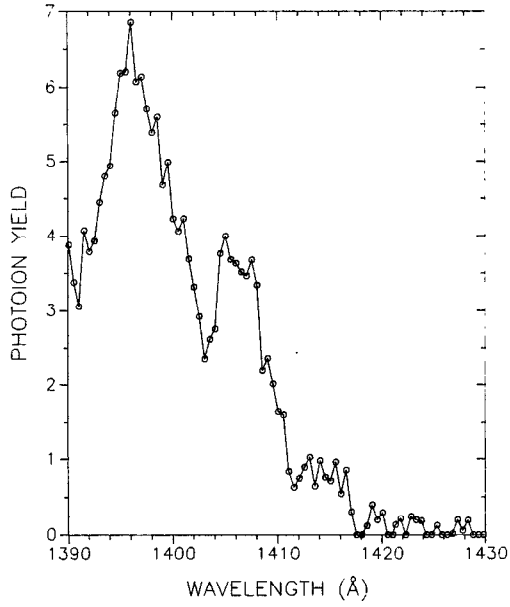

FIG. 7. The threshold region of the photoion yield curve of SbH^+ (SbH).

C. SbH

The photoion yield curve of SbH^+(SbH) from ~1180–1430 Å is presented in Fig. 6. The first indication of a signal above background is a small step at 1416.5±1.5 Å≡8.753±0.009 eV (see Fig. 7), which is probably the adiabatic IP, corresponding to the process

$$SbH(X\,^3\Sigma^-,0^+)+h\nu\rightarrow SbH^+(X\,^2\Pi_{1/2})+e.$$

However, there is a caveat. One must consider the possibility that this initial weak step may correspond to ionization of the excited ($\Omega=1$) component of $^3\Sigma^-$, lying ~655 cm^{-1}≡0.0812 eV (Ref. 9) higher than 0^+. In the vast majority of cases studied with this source (with one exception), the species observed could be characterized as being equilibrated at about room temperature. For SbH ($\Omega=1$), with a degeneracy of 2, its abundance relative to SbH (0^+) would be predicted to about 8%. The observed intensity of the 1416 Å feature to the contiguous peak at shorter wavelength is about 20%. Also, this next feature appears at about 1410 Å, which is 0.04 eV to higher energy, rather than 0.08 eV. Hence, in all likelihood the adiabatic IP is 8.75 eV, but it could conceivably be as high as 8.79 eV.

The photoion yield curve of Fig. 6 bears some resemblance to the results of earlier experiments on PH^+(PH) and AsH^+(AsH), although this conclusion requires some perspicacity. Autoionization structure is prominent in all three cases. With PH and AsH, it was possible to assign the autoionizing peaks to Rydberg series converging to the $a\,^4\Sigma^-$ excited state, lying about 2 eV above the ground state of the cation. SbH^+ is isoelectronic with SnH, which has an excited $a\,^4\Sigma^-$ state lying about 2 eV about the ground ($^2\Pi_r$) state.[9] Hence, a plausible approach is to find Rydberg progressions among the observed peaks which converge to a limit ~10.8 eV.

A list of the observed features is given in Table I. The three largest peaks occur at 1378.5±0.8, 1255±1, and 1210±1 Å. With a limit of 10.866±0.011 eV, these features approximately conform to the Rydberg formula

$$E_n=\mathrm{IP}-\frac{R}{(n^*)^2},$$

with n^*=2.696, 3.713, and 4.687, respectively. Two members of another series (broad features at 1282±1 and 1221±1 Å) appear to conform to this limit, with n^*=3.374 and 4.372. However, the two sharper peaks (at 1316±1 and 1236±1 Å) appear to fit better to a slightly lower limit, 10.843±0.011 eV, with resulting n^* values of 3.093 and 4.093. That there may exist two limits is not surprising, since $^4\Sigma^-$ can be expected to split in Hund's case (c) into 1/2 and 3/2 components, differing by 6 λ, where λ is the spin–spin interaction constant. If we approximate λ by the value observed in the $a\,^4\Sigma^-$ state of the isoelectronic SnH molecule (45.78 cm^{-1}),[9,21] we arrive at a 1/2–3/2 splitting of 275 cm^{-1}≡0.034 eV, which is close to the difference (0.023±0.015) of the limits arrived at from the autoionizing peaks. Two additional peaks, at

TABLE I. Rydberg series members observed in SbH.

λ (Å)	E (eV)	n^* (IP=10.843±0.011 eV)	n^* (IP=10.866±0.011 eV)
Tentatively assigned features			
1378.5±0.8	8.994±0.005		2.696
1255±1	9.879±0.008		3.713
1210±1	10.247±0.008		4.687
1282±1	9.671±0.008		3.374
1221±1	10.154±0.008		4.372
1316±1	9.421±0.007	3.093	
1236±1	10.031±0.008	4.093	
1406±1	8.818±0.006	2.592	(2.577)
1266±1	9.793±0.008	3.600	(3.561)
Unassigned features			
1396.5±1.0	8.878±0.006		
1371.5±0.8	9.040±0.005		
1364.5±0.8	9.086±0.005		
1207.5±0.5	10.268±0.004		

TABLE II. Adiabatic ionization potentials of the pnicogen hydrides.

	PnH			PnH_2			PnH_3	
	Expt.	Calc.		Expt.	Calc.		Expt.	Calc.
NH	13.49±0.01[a]	13.48[b]	$NH_2(^3B_1)$	11.14±0.01[c]	11.20[b]	NH_3	10.1864±0.0001[e]	10.19[f]
			$(^1A_1)$	12.445±0.002[c]	12.46[c]			
PH	10.149±0.008[g]	10.09[f]	PH_2	9.824±0.002[h]	9.72[f]	PH_3	9.870[h]	9.87[f]
							9.868±0.005[i]	
AsH	9.641±0.008[j]	9.69[k]	AsH_2	9.443±0.007[j]	9.39[k]	AsH_3	9.82±0.01[j]	9.53[k]
		(9.40)[l]			9.25[l]			9.50[l]
SbH	8.753±0.009[m]	(8.45)[l]	SbH_2	8.731±0.012[m]	8.38	SbH_3	9.40±0.02[m]	8.90[l]

[a]S. J. Dunlavey, J. M. Dyke, N. Jonathan, and A. Morris, Mol. Phys. **39**, 1121 (1980).
[b]Reference 18.
[c]Reference 15.
[d]L. A. Curtiss and J. A. Pople, J. Chem. Phys. **90**, 603 (1989).
[e]Combining IP to $v_2' = 1$ from W. Habenicht, G. Reiser, and K. Müller-Dethlefs, J. Chem. Phys. **95**, 4809 (1991) with $\Delta(v_2' = 0 \rightarrow 1)$ from S. S. Lee and T. Oka, J. Chem. Phys. **94**, 1698 (1991).
[f]L. A. Curtiss, K. Raghavachari, G. W. Trucks, and J. A. Pople, J. Chem. Phys. **94**, 7221 (1991).
[g]Reference 8(b).
[h]Reference 8(a).
[i]R. Maripuu, I. Reineck, H. Ågren, N.-Z. Wu, J. M. Rong, H. Veenhuizen, S. H. Al-Shamma, L. Karlsson, and K. Siegbahn, Mol. Phys. **48**, 1255 (1983).
[j]Reference 7.
[k]R. C. Binning, Jr. and L. A. Curtiss, J. Chem. Phys. **92**, 3688 (1990).
[l]Reference 6. The value for IP (AsH) given by these authors is for the transition AsH ($X\,^3\Sigma^-$) to AsH^+ ($X\,^2\Pi$). The measured IP (AsH) is from AsH ($X\,0^+$) to AsH^+ ($X\,^2\Pi_{1/2}$). For the latter, the spin–orbit splitting is about 0.2 eV ($^2\Pi_{1/2}$–$^2\Pi_{3/2}$), whereas the 0^+–1 zero field splitting is $\sim 0.01_5$ eV. The effect of these corrections is to reduce the IP (AsH) given by Dai and Balasubramanian (9.50 eV) to about 9.40 eV. A similar correction is made for IP (SbH), where ξ (Sb) $\approx$ 0.422 eV, ξ (Sb^+) $\approx$ 0.468 eV and the zero field splitting is 0.08 eV.
[m]Present results.

1406±1 and 1266±1 Å, appear to be components of a series converging to the lower limit (n^*=2.592 and 3.600), although they could conceivably be associated with the upper limit (n^*=2.577 and 3.561).

Note that the value of λ chosen for SbH^+ ($a\,^4\Sigma^-$) is much smaller (45.78 cm^{-1}) than the value of λ chosen for SbH ($X\,^3\Sigma^-$), 333.39 cm^{-1}.[9] A similar relationship exists between λ for GeH ($a\,^4\Sigma^-$), which is 6.52 cm^{-1},[9] and λ for AsH ($X\,^3\Sigma^-$), which is 58.87 cm^{-1}.[9] Consequently, the limit previously observed for AsH^+($a\,^4\Sigma^-$) (Ref. 7) may actually be split by $\sim$39 $cm^{-1} \equiv 0.005$ eV.

A portion of the difference between the λ for $^4\Sigma^-$ and that for $^3\Sigma^-$ appears to be a matter of definition. Kovacs[22] uses the parameter ε while Herzberg[23] prefers λ. If one compares their formulas for $^3\Sigma^-$, one finds that the more conventionally used $\lambda = 3/2\ \varepsilon$. However, if one compares the $^4\Sigma^-$ formulas in Kovacs[22] and Klynning *et al.*,[21] ε is actually the λ reported for SnH and GeH. Hence, if one uses a more consistent definition of the spin–spin interaction parameter, it differs between $^3\Sigma^-$ (SbH) and $^4\Sigma^-$ (SnH) by a factor 4.85, and for $^3\Sigma^-$ (AsH) and $^4\Sigma^-$ (GeH) by a factor 6.02. We speculate that the large difference between λ (or ε) in $^3\Sigma^-$ and $^4\Sigma^-$ states of related molecules is a consequence of the molecular orbital structure of these states. For $^3\Sigma^-$, the molecular orbital description is $\sigma^2\pi^2$, and the spin splitting occurs between the two electrons in the single π orbital. For $^4\Sigma^-$, the molecular orbital description is $\sigma\pi^2$, and the spin splitting is an average among two σ–π interactions and the π–π interaction.

IV. DISCUSSION

A. The ionization potentials

In Table II, we summarize the adiabatic ionization potentials determined in the present work, and compare them with the *ab initio* calculated values of Dai and Balasubramanian.[6] Also shown are the results, both experimental and calculational, of the adiabatic ionization potentials of the other Group V mono and di-hydrides. For NH_2, we list the IP to the excited $^1A_1$ state, so that it may be compared to the other di-hydrides, where $^1A_1$ is the ground state of the cation. For NH, NH_2, PH, and PH_2, AsH and AsH_2, the experimental values are known to accuracies of $\leqslant$0.01 eV, and the calculated values of Pople, Curtiss, and collaborators agree to within ±0.10 eV. For AsH and AsH_2, there also exist calculated values by Dai and Balasubramanian, which differ from experiment by $\sim$0.24 and 0.19 eV, respectively. The antimony hydrides are currently too heavy to be treated by the *ab initio* methods of Pople, Curtiss *et al.* The calculated values of Dai and Balasubramanian differ from our experimental values by $\sim$0.30 eV (SbH) and $\sim$0.35 eV (SbH_2). For SbH_3, the calculation differs by $\sim$0.5 eV from our value, and 0.6 eV from the photoelectron spectroscopic value, but since this transition involves an extended Franck–Condon region, it is conceivable that the experimental results do not reach the adiabatic threshold, in which case the deviation would be diminished.

We had shown previously[7] that the Goddard–Harding

TABLE III. Experimental ionization energies (eV) of pnicogen hydrides (modified by spin–orbit splittings), their differences Δ, and the value Δ′ based on a Goddard–Harding-like model.

	IP(Pn)[a]	Δ	IP(PnH)[b]	Δ	$IP(PnH_2)$	$\Delta'=K/2$[c]
N	14.560	1.07	13.49	1.045	12.445	0.397
P	10.526	0.359	10.167	0.343	9.824	0.235
As	10.0076	0.271	9.736	0.293	9.443	0.223
Sb	9.124	0.184	8.94	0.21	8.731	0.190

[a]The IP(Pn) given here is the energy of the hypothetical transition between $Pn(^4S)$ and $Pn^+(^3P)$, where the latter is the weighted mean of $^3P_{0,1,2}$. The sources of data are N[C. E. Moore, *Atomic Energy Levels*, NSRDS-NBS35, NBS Circular 467 (U.S. Printing Office, Washington, D.C.)]; P [W. C. Martin, J. Opt. Soc. Am. **49**, 1071 (1959)]; As [K. S. Bhatia and W. E. Jones, Can. J. Phys. **49**, 1773 (1971) and H. Li and K. L. Andrew, J. Opt. Soc. Am. **61**, 96 (1971)]; Sb [W. E. Jones and J. M. Martell, Can. J. Phys. **69**, 891 (1991) and B. Arcimowicz, Y. N. Joshi, and V. Kaufman, Can. J. Phys. **67**, 572 (1989)].

[b]The IP(PnH) given here is from $PnH(X\,^3\Sigma^-)$ to $PnH^+(X\,^2\Pi)$. Hence, the experimental value, which corresponds to formation of $PnH^+(X\,^2\Pi_{1/2})$, is increased by $\frac{1}{2}\zeta$(Pn), and slightly decreased by the weighted zero field splitting of PnH $(X\,^3\Sigma^-)$.

[c]The two lowest LS states of Pn, ^4S and ^2D, differ by $3K$. Thus K is evaluated from the difference in these energies, after computing the weighted mean of $^2D_{5/2,3/2}$.

approach could be extended to predict the difference in ionization energies. The difference between the ionization energies of Pn and PnH was also the difference between PnH and PnH_2, and found to be $-J+J'-K+K'/2$, where the J's and K's are coulomb and exchange integrals involving different combinations of p_x, p_y, and p_z orbitals of Pn (Pn=N, P, As, Sb). In the approximation where all the J's are equal, and all the K's are equal, this difference becomes $K/2$, the same quantity by which the consecutive bond energies were predicted to differ by Goddard and Harding. In Table III, we compare the predictions of this semiempirical model with the present results, and the earlier work on nitrogen, phosphorus, and arsenic hydrides. Since the model does not include spin–orbit effects, but the experimental results implicitly involve them, it is necessary to modify the latter to make the comparisons more valid. Thus the process $Pn(^4S)\rightarrow Pn^+$ occurs to $^3P_{0,1,2}$. Our modified IP is to the center of gravity of ^3P. Similarly, PnH $(^3\Sigma^-)\rightarrow PnH^+$ can form $X\,^2\Pi_{1/2}$ and $^2\Pi_{3/2}$, separated approximately by ξ, the spin–orbit constant of Pn. Our modified IP in this case is the mean of $^2\Pi_{1/2}$ and $^2\Pi_{3/2}$. Finally, there remains the zero field splitting of PnH $(^3\Sigma^-)$ into 0^+ and 1 states, which begins to be noticeable in AsH, and is significant in SbH.

Using the adjusted ionization potentials, we note that the difference in IP's between Pn and PnH is very nearly the difference between the IP's of PnH and PnH_2, bearing out one prediction of the model. However, the absolute magnitude of this difference is larger than $K/2$; for N, the observed difference is about 1.05 eV, whereas $K/2\cong 0.4$ eV. This discrepancy diminishes significantly for P, and monotonically thereafter, until it almost vanishes for Sb ($\sim$0.20 eV observed, 0.19 eV predicted). The large discrepancy for N, which also appears in the consecutive bond energies, has been discussed previously.[7] The good agreement for Sb provides at least heuristic support for the experimental IP's reported here. The fact that ΔIP(Pn–PnH) and $\Delta IP(PnH–PnH_2)$ are nearly equal, but the absolute values differ from $K/2$, may be evidence for the view that the assumptions $J=J'$ and $K=K'$ are not quite valid.

B. The bond energies

The fragmentation process that occurs at lowest energy in the photodissociative ionization of SbH_3 (and hence the most thermochemically significant, in principle) is

$$SbH_3+h\nu\rightarrow SbH^+ + H_2 + e,$$

with a 0 K threshold at $9.73_0\pm 0.008$ eV. If we subtract the currently measured IP(SbH) $=8.753\pm 0.009$ eV, we obtain an endothermicity of 0.977 ± 0.012 eV$\equiv 22.5\pm 0.3$ kcal/mol for the corresponding neutral process,

$$SbH_3\rightarrow SbH + H_2.$$

In combination with $\Delta H^0_{f0}(SbH_3)=36.54\pm 0.10$ kcal/mol,[1] we readily obtain $\Delta H^0_{f0}(SbH)=59.1\pm 0.3$ kcal/mol, or [with ΔH^0_{f0}(Sb) and ΔH^0_{f0}(H) given in Sec. I], $D_0(SbH)=56.4\pm 1.0$ kcal/mol. Using $D_0(H_2)=4.4781_3$ eV,[9] the endothermicity for the upper process yields the sum of the other two bonds, which is 125.8 ± 0.3 kcal/mol.

The fragmentation process

$$SbH_3+h\nu\rightarrow SbH_2^+ + H + e$$

was found to have a 0 K onset at 11.66 ± 0.02 eV. By subtracting $IP(SbH_2)=8.731\pm 0.012$ eV, given in Sec. III B, we obtain 2.929 ± 0.02 eV$\equiv 67.5\pm 0.5$ kcal/mol for $D_0(H_2Sb–H)$. Therefore, the energy of the remaining bond, D_0(HSb–H), must be $125.8–67.5=58.3\pm 0.6$ kcal/mol, corresponding to $\Delta H^0_{f0}(SbH_2)=52.5\pm 0.6$ kcal/mol. These bond energies, together with the semiempirical predictions of Goddard and Harding and the *ab initio* calculations of Dai and Balasubramanian are summarized in Table IV.

Although the *ab initio* bond energies of Dai and Balsubramanian are uniformly lower than the experimental values (and therefore do not sum to the expected atomization energy of SbH_3), they predict a deviation from equal increments ($\Delta'=K/2$) which is observed experimentally, and in the same direction. D_0(Sb–H) is closer to D_0(HSb–H) than predicted by the semiempirical model, and there is a larger gap between D_0(HSb–H) and $D_0(H_2Sb–H)$. As mentioned in Sec. I, this pattern was beginning to be evident in the corresponding arsenic hydrides.

We must first consider whether this deviation from the Goddard–Harding model can be an artifact of our experimental procedure. One feature common to our studies of PH_n, AsH_n, and SbH_n is that the lowest energy fragmentation process from PnH_3 forms $PnH^+ + H_2 + e$. The higher energy fragmentation, which forms $PnH_2^+ + H + e$, may be subject to a kinetic shift. If this were the case, our inferred value of $D_0(H_2Pn–H)$ would be higher than the true value, and the consequent allocation of the consecutive bond energies would deviate from the Goddard–Harding predictions in the observed fashion. However, our experimental values for $D_0(H_2Pn–H)$ agree very well with

TABLE IV. Comparison of experimental Sb–H_n bond energies with semiempirical predictions and *ab initio* calculations (in kcal/mol at 0 K).

Bond	Semiempirical[a]	$\Delta'=K/2$	*Ab initio*[b]	Δ	Expt.[c]	Δ
$D_0(H_2Sb-H)$	65.17		63.3		67.5±0.5	
		4.44		7.5		9.2±0.8
$D_0(HSb-H)$	60.73		55.8		58.3±0.6	
		4.44		1.9		1.9±1.2
$D_0(Sb-H)$	56.29		53.9		56.4±1.0	

[a]From Ref. 3. The values differ slightly from the ones given by Goddard and Harding, because of a more recent value for ΔH^0_{f0} (Sb) used in the present work.
[b]From Ref. 6.
[c]Present results.

both the Goddard–Harding predictions and *ab initio* calculations for $D_0(H_2P-H)-82.5\pm0.5$ kcal/mol experiment, 81.11 kcal/mol semiempirical, 82.4 kcal/mol *ab initio*; and $D_0(H_2As-H)-74.9\pm0.2$ kcal/mol experiment, 74.89 kcal/mol semiempirical, 74.6 kcal/mol *ab initio*. With SbH_3, there is a smaller energy gap between AP (SbH^+) and AP (SbH_2^+), making the possibility of a kinetic shift less likely. The formation of SbH_2^+ (and the other PnH_2^+) involves a simple bond rupture, whereas the formation of $SbH^+ + H_2$ involves a more constrained transition state, as noted in Sec. III. Finally, there is some theoretical support for this deviation from the Goddard–Harding model in the *ab initio* calculations of Dai and Balasubramanian. Therefore, we conclude that the effect is real.

Goddard and Harding[3] assumed "each bond pair to be purely covalent." A conceivable cause for the observed deviation is a departure from this premise. The degree of ionicity can be estimated from the difference in electronegativity in the bond pair. For H, the electronegativity[24] is 2.1, while for N, P, As, and Sb it is 3.0, 2.1, 2.0, and 1.9. Clearly, the largest deviation from purely covalent behavior is N–H, and this may explain the large discrepancy between the absolute values of the observed gaps Δ and the predicted ones $\Delta'=K/2$ for the nitrogen hydrides, both in their ionization and dissociation behavior. However, this effect seems to be a small one when examining the *differences* between gaps, i.e., $D_0(H_2Pn-H)$-$D_0(HPn-H)$ vs $D_0(HPn-H)-D_0(Pn-H)$. A more likely cause is a heavy element effect, manifested by spin–orbit or relativistic behavior.

We can invoke a simple model to rationalize the observed departure from the Goddard–Harding model. In the limit of pure j–j coupling, the p orbital splits into a $p_{1/2}$ orbital (which can be occupied by two electrons) and a $p_{3/2}$ orbital, somewhat less bound, which can accommodate up to four electrons. The pnicogen atoms all have three valence p electrons. These can be visualized as being distributed, two in the $p_{1/2}$ subshell and one in the $p_{3/2}$ subshell. This latter electron is the one which can most readily form a bond. The resulting ground state of PnH is $^3\Sigma^-$ for NH and PH. Both molecules conform to Hund's case (b), with $B/\lambda=17.8$ and 3.8 for NH and PH, respectively[25] (where B is the rotational constant and λ is the spin–spin interaction parameter). For AsH,[25] SbH,[3] and BiH,[9] $B/\lambda=0.12$, 0.017, and 0.0015, as the coupling scheme moves progressively to Hund's case (c). For these latter molecules, a splitting of the $^3\Sigma^-$ into 0^+ (ground state) and 1 (excited state) is manifest, and increases from ~100 cm^{-1} (AsH) to ~650 cm^{-1} (SbH) to ~4900 cm^{-1} (BiH).[9] Addition of a second H atom to PnH in these heavier species requires some promotional energy, to break the pairing in the 0^+ state (which is analogous to the $p_{1/2}$ subshell in the atomic case). Consequently, the net bond energy for this second bond will be correspondingly reduced. The third bond can be formed with no additional promotional energy. Upon examining the behavior of the As–H_n bonds and the Sb–H_n bonds, it appears as if this second bond energy is the one most deviant from the Goddard–Harding picture, as predicted by this simple model.

If this model were to be extrapolated to the bismuth hydrides, it would very likely predict a reversal, i.e., $D_0(BiH) > D_0(HBi-H)$. This is not reflected in the calculations of Dai and Balasubramanian,[6] who calculate $D_0(BiH)=41.0$ kcal/mol and $D_0(HBi-H)=45.4$ kcal/mol. Other evidence suggests that this reversal may indeed occur. The heat of formation of BiH_3 is poorly known. Gunn[26] has estimated $\Delta H^0_{f298}(BiH_3)=55$ kcal/mol, based on extrapolation. Saalfeld and Svec[27] give $\Delta H^0_{f298}(BiH_3)=66$ kcal/mol, based on the electron impact appearance potential of Bi^+ (BiH_3). Modern concepts of kinetic shifts make this value highly suspect. The corresponding values at 0 K would be 57 and 68 kcal/mol,[28] leading to atomization energies of 148 kcal/mol (Gunn) and 137 kcal/mol (Saalfeld and Svec). The sum of the individual bond energies (i.e., the atomization energy) calculated by Dai and Balasubramanian [6] is 138.2 kcal/mol. Their calculations tend to give lower bond energies than experiment. In the case of SbH_3, their atomization energy is $\sim95\%$ of the experimental value. Applying this figure to BiH_3, one obtains an atomization energy of 145.5 kcal/mol, reasonably close to the value based on Gunn's estimate of ΔH^0_{f298} (BiH_3).

Lindgren and Nilsson[29] have observed a predissociation in the $E0^+$, $v'=2$ state of BiH, at 38,425 cm^{-1}. Their inference was that the products of this dissociation were $Bi(^2D_{3/2})+H(^2S)$, which would imply $D_0(BiH)\leqslant34\,825-11\,419=23\,406$ cm$^{-1}\equiv2.90$ eV. On the basis of *ab initio* calculations, Balasubramanian[30] has concluded that the

products of this predissociation are $Bi(^2D_{5/2})+H(^2S)$, and hence $D_0(BiH) \leqslant 34\,825-15\,438$ (Ref. 4) $=19\,387$ $cm^{-1} \equiv 2.40$ eV. Lindgren and Nilsson[29] note that "it seems likely that the exact value of the dissociation energy is found not far from the given upper limit." Thus accepting the interpretation of Balasubramanian,[30] $D_0(BiH) \sim 2.4$ eV $\equiv 55$ kcal/mol, and the sum of the other two bonds in BiH_3 would be about 93 kcal/mol. If this latter quantity were equally partitioned between D_0(HBi–H) and $D_0(H_2Bi–H)$, the first bond, i.e., $D_0(BiH)$, would be about 9 kcal/mol stronger than the second. On the basis of the Goddard–Harding model, $D_0(H_2Bi–H)$ is probably larger than D_0(HBi–H), and hence $D_0(BiH)$ should exceed D_0(HB–H) by more than 9 kcal/mol. The higher value of $\Delta H^0_{f298}(BiH_3)$ given by Saalfeld and Svec[27] would exacerbate this difference, but (as mentioned earlier) this result is highly questionable.

It is an interesting exercise to try to modify the Goddard–Harding model by incorporating relativistic effects, which are expected to be dominant in the BiH_n system. In the simplest approach, the difference between the third and second bond energy remains $K/2$, but D_0(HBi–Hi)$-D_0$(Bi–H) $\approx K/2-\Delta E$, where ΔE is the promotional energy necessary to make the relativistic coupled electron pair in BiH ($\tilde{X}0^+$) available for bonding. Approximating ΔE by the 0^+-1 splitting in BiH (~ 4900 cm^{-1}),[19] we arrive at D_0(HBi–H)$-D_0$(BiH) $\approx 6.6-14.0=-7.5$ kcal/mol, while $D_0(H_2Bi–H)-D_0$(HBi–H) ≈ 6.6 kcal/mol. Using the atomization energy of BiH_3, the individual bonds are calculated to be 51.2 ($H_2Bi–H$), 44.6 (HBi–H), and 52.1 kcal/mol (Bi–H). The latter value is fortuitously close to the spectroscopically derived $D_0(BiH) \approx 55$ kcal/mol discussed above. More importantly, however, even this simple relativistic correction to the Goddard–Harding model predicts that D_0(Bi–H) $> D_0$(HBi–H). In the case of SbH_n, the analogous relativistic correction is much smaller, and does not reverse the ordering of bond energies, which become 64.6 ($H_2Sb–H$), 60.1 (HSb–H), and 57.5 kcal/mol (Sb–H).

A possible manifestation of the relativistic effect can be seen in the pnicogen fluorides. These systems do not conform to the Goddard–Harding model. In fact,[31] D_0(N–F) $> D_0$(FN–F) $> D_0(F_2N–F)$, just the reverse of the order given by Goddard and Harding for the consecutive bond energies in the NH_n system. The weakening of the N–F bond energies with addition of fluorine atoms has been attributed at least partly to repulsion of the negatively charged fluorine valence orbitals. These repulsions can be expected to be stronger for first row compounds like N–F than for heavier ones, since the internuclear distances are shorter. In fact, the sequence of P–F bonds[31] becomes the same as for P–H bonds, i.e., $D_0(F_2P–F) > D_0$(FP–F) $> D_0$(P–F). Lack of information on As–F and Sb–F bonds prevents us from testing the progressive behavior of these consecutive bond energies. However, recent studies from our laboratory on the BiF_n system[32] demonstrate that $D_0(BiF)=3.76\pm0.13$ eV is larger than D_0(FBi–F) $=3.50 \pm 0.15$ eV, and $D_0(F_2Bi–F)=4.5_1$, ± 0.2 eV is the largest of these bonds. Hence, it may be that the relativistic effect in the bismuth fluorides has enabled D_0(Bi–F) to overtake D_0(FBi–F), as we tentatively predict for the corresponding bond energies in the BiH_n system.

ACKNOWLEDGMENT

This work was supported by the U.S. Department of Energy, Office of Basic Energy Sciences, under Contract No. W-31-109-ENG-38.

[1] S. R. Gunn, W. L. Jolly, and L. G. Green, J. Phys. Chem. **64**, 1334 (1960).
[2] R. K. Yoo, B. Ruscic, and J. Berkowitz, J. Electron Spectrosc. (in press) (in particular, see Table 5 and Ref. 39 therein).
[3] W. A. Goddard III and L. B. Harding, Annu. Rev. Phys. Chem. **29**, 363 (1978).
[4] C. E. Moore, Natl. Bur. Stand. (U.S.), Circ. 467.
[5] A summary of the results of L. A. Curtiss, J. A. Pople, and collaborators for NH_n, PH_n, and ASH_n bond energies appears in Table ii of J. Berkowitz and B. Ruscic, in *Vacuum Ultraviolet Photoionization and Photodissociation of Molecules and Clusters*, edited by C. Y. Ng (World Scientific, Singapore, 1991), p. 10.
[6] D. Dai and K. Balasubramanian, J. Chem. Phys. **93**, 1837 (1990).
[7] J. Berkowitz, J. Chem. Phys. **89**, 7065 (1988).
[8] (a) J. Berkowitz, L. A. Curtiss, S. T. Gibson, J. P. Greene, G. L. Hillhouse, and J. A. Pople, J. Chem. Phys. **84**, 375 (1986); (b) J. Berkowitz and H. Cho, *ibid.* **90**, 1 (1989).
[9] K. P. Huber and G. Herzberg, *Molecular Spectra and Molecular Structure IV. Constants of Diatomic Molecules* (Van Nostrand, New York, 1979).
[10] W. L. Jolly and J. E. Drake, *Inorg. Synthes.*, Vol. VII (McGraw-Hill, New York, 1963), pp. 43–44.
[11] B. Ruscic, J. P. Greene, and J. Berkowitz, J. Phys. B **17**, 1503 (1984).
[12] B. Ruscic and J. Berkowitz, Phys. Rev. Lett. **50**, 675 (1983).
[13] A. W. Potts and W. C. Price, Proc. R. Soc. London Ser. A **326**, 181 (1972).
[14] See P. M. Guyon and J. Berkowitz, J. Chem. Phys. **54**, 1814 (1971). The vibrational frequencies of SbH_3 are given by W. H. Haynie and H. H. Nielsen, J. Chem. Phys. **21**, 1839 (1953).
[15] S. T. Gibson, J. P. Greene, and J. Berkowitz, J. Chem. Phys. **83**, 4319 (1985).
[16] K. Dressler and D. A. Ramsay, Phil. Trans. R. Soc. London, Ser. A **251**, 553 (1959); J. Chem. Phys. **27**, 971 (1957).
[17] J. A. Pople, B. T. Luke, M. J. Frisch, and J. S. Binkley, J. Phys. Chem. **89**, 2198 (1985).
[18] J. A. Pople and L. A. Curtiss, J. Phys. Chem. **91**, 155 (1987).
[19] K. Balasubramanian, J. Chem. Phys. **91**, 2443 (1989).
[20] P. Jensen, P. R. Buenker, and A. D. McLean, Chem. Phys. Lett. **141**, 53 (1987); M. Okumura, B. D. Rehfuss, B. M. Dinelli, M. G. Bawendi, and T. Oka, J. Chem. Phys. **90**, 5918 (1989).
[21] L. Klynning, B. Lindgren, and N. Åslund, Ark. Fys. **30**, 141 (1965).
[22] I. Kovacs, *Rotational Structure in the Spectra of Diatomic Molecules* (Elsevier, New York, 1969), p. 85.
[23] G. Herzberg, *Molecular Spectra and Molecular Structure. I. Spectra of Diatomic Molecules* (Van Nostrand, New York, 1950).
[24] The electronegativities are taken from L. Pauling, *The Nature of the Chemical Bond*, 3rd ed. (Cornell University, Ithaca, 1960), pp. 90, 93.
[25] J. R. Anacona, P. B. Davies, and S. A. Johnson, Mol. Phys. **56**, 989 (1985).
[26] S. R. Gunn, J. Phys. Chem. **68**, 949 (1964).
[27] F. E. Saalfeld and H. J. Svec, Inorg. Chem. **2**, 46 (1963).
[28] A. S. Yushin and V. S. Mikheev, Zh. Fiz. Khim. **48**, 488 (1974).
[29] B. Lindgren and Ch. Nilsson, J. Mol. Spectrosc. **55**, 407 (1975).
[30] K. Balasubramanian, J. Mol. Spectrosc. **115**, 258 (1986).
[31] J. Berkowitz, J. P. Greene, J. Foropoulos, Jr., and O. M. Neskovic, J. Chem. Phys. **81**, 6166 (1984).
[32] R. K. Yoo, B. Ruscic, and J. Berkowitz, Chem. Phys. **166**, 215 (1992).